APPLIED AND ENVIRONMENTAL MICROBIOLOGY, Dec. 2002, p. 6332–6342 Vol. 68, No. 12
0099-2240/02/$04.00+0 DOI: 10.1128/AEM.68.12.6332–6342.2002

Effect of Different NADH Oxidase Levels on Glucose Metabolism by *Lactococcus lactis*: Kinetics of Intracellular Metabolite Pools Determined by In Vivo Nuclear Magnetic Resonance

Ana Rute Neves,[1] Ana Ramos,[1] Helena Costa,[1] Iris I. van Swam,[2] Jeroen Hugenholtz,[2] Michiel Kleerebezem,[2] Willem de Vos,[2] and Helena Santos[1]*

Instituto de Tecnologia Química e Biológica/Universidade Nova de Lisboa and Instituto de Biologia Experimental e Tecnológica, 2780-156 Oeiras, Portugal,[1] and Wageningen Centre for Food Sciences Food Research/NIZO, 6710 BA Ede, The Netherlands[2]

Received 13 May 2002/Accepted 5 September 2002

Three isogenic strains of *Lactococcus lactis* with different levels of H_2O-forming NADH oxidase activity were used to study the effect of oxygen on glucose metabolism: the parent strain *L. lactis* MG1363, a NOX^- strain harboring a deletion of the gene coding for H_2O-forming NADH oxidase, and a NOX^+ strain with the NADH oxidase activity enhanced by about 100-fold. A comprehensive description of the metabolic events was obtained by using ^{13}C nuclear magnetic resonance in vivo. The most noticeable results of this study are as follows: (i) under aerobic conditions the level of fructose 1,6-bisphosphate [Fru(1,6)P_2] was lower than the level under anaerobic conditions, and the rate of Fru(1,6)P_2 depletion was very high; (ii) the levels of 3-phosphoglycerate and phosphoenolpyruvate were considerably enhanced under aerobic conditions and significantly lower in the NOX^- strain; and (iii) the glycolytic flux decreased in the presence of saturating levels of oxygen, but it was not altered in response to changes in the NADH oxidase activity. In particular, the observation that the glycolytic flux was not enhanced in the NOX^+ strain indicated that glycolytic flux was not primarily determined by the level of NADH in the cell. The patterns of end products were identical for the NOX^- and parent strains; in the NOX^+ strain the carbon flux was diverted to the production of α-acetolactate-derived compounds, and at a low pH this strain produced diacetyl at concentrations up to 1.6 mM. The data were integrated with the goal of identifying the main regulatory aspects of glucose metabolism in the presence of oxygen.

Lactococcus lactis is a facultatively anaerobic bacterium that converts more than 90% of milk sugar to lactate, preventing spoilage of fermented foods. Although this organism exhibits relatively simple carbohydrate metabolism, primarily designed for energy conservation, considerable versatility with respect to end product formation has been described (26). The pattern of end products resulting from glucose metabolism under anaerobic conditions, characterized by the production of large amounts of lactate and only trace amounts of acetate, ethanol, formate, and 2,3-butanediol, is markedly different from that observed in the presence of oxygen. In fact, when the organism is switched from an anaerobic atmosphere to an aerobic atmosphere, a mixture of lactate and acetate is produced, and enhancement of the flux through α-acetolactate synthase is observed, resulting in acetoin-diacetyl production (7, 8, 28, 40). Diacetyl is a by-product of aerobic metabolism with industrial relevance, since it confers the butter-like taste characteristic of many dairy foods; this trait was the basis for several previous studies that focused on strategies to enhance diacetyl production (16, 22). Nevertheless, the mechanisms involved in regulation of the metabolic switch from homolactic fermentation to mixed acid and aroma fermentation under aerobic conditions are not completely understood.

The ability of *L. lactis* to grow under aerobic conditions has been correlated with the presence of the flavoproteins NADH oxidase and NADH peroxidase and a manganese-containing superoxide dismutase (SOD) (8, 17, 36). Recently, the H_2O-forming NADH oxidase has been shown to play an important role in the aerobic metabolism of *L. lactis* and *Streptococcus mutans*, since it contributes to the regeneration of NAD^+ during the metabolism of carbohydrates (19, 28). Additionally, overexpression of *S. mutans* H_2O-forming NADH oxidase in *L. lactis* resulted in a substantial redirection in the carbon flux towards the formation of acetate and acetoin (27). Therefore, a key role for NADH and NAD^+ levels (or the internal redox state) in the regulation of carbohydrate metabolism has been postulated (15, 21, 24, 32, 33).

To extend our knowledge about the regulatory mechanisms underlying the metabolic shift in the presence of oxygen, we used in vivo ^{13}C nuclear magnetic resonance (^{13}C-NMR) to characterize intracellular metabolite pools in a noninvasive way. The power of this technique to elucidate different aspects of microbial metabolism has been amply demonstrated (6, 10, 11, 32, 33, 39). Because of the great impact that the capacity to regenerate NAD^+ has on the metabolic pattern of *L. lactis*, it was deemed important to manipulate this capacity by knocking out the gene encoding an H_2O-forming NADH oxidase (NOX^- construct) or by overexpressing the homofunctional gene from *S. mutans* (NOX^+ construct). The dynamics of intracellular pools of key glycolytic metabolites, the patterns of end products, and the levels of relevant glycolytic activities in the presence or absence of oxygen are discussed below in relation to the levels of NADH oxidase in the two engineered strains, as well as in strain MG1363.

* Corresponding author. Mailing address: Instituto de Tecnologia Química e Biológica, Universidade Nova de Lisboa, Rua Da Quinta Grande, 6, Apt. 127, 2780-156 Oeiras, Portugal. Phone: 351-214469828. Fax: 351-214428766. E-mail: santos@itqb.unl.pt.

MATERIALS AND METHODS

Organisms used and plasmid construction. *L. lactis* MG1363 and two derivative strains were used throughout this study. The NOX^+ strain was obtained by transformation of *L. lactis* NZ3900 with plasmid pNZ2600, a derivative of pNZ8020 containing the water-forming NADH oxidase encoded by the *nox-2* gene of *S. mutans* under control of the lactococcal *nisA* promoter (27). Strain NZ3900 is an MG1363 derivative which contains the *nisRK* genes integrated in the chromosome, which allows nisin-controlled expression of the *nox-2* gene (12). The NOX^- strain is a derivative of MG1363 carrying a deletion of *nox-2* (or the *noxE* gene of *L. lactis*). Cloning of the *nox-2* gene of *L. lactis* MG1363, which encodes the major water-forming NADH oxidase, was recently described (20) (GenBank accession no. AY046926). The chromosomal *nox-2* gene was knocked out in *L. lactis* MG1363 by using a double-crossover gene disruption strategy. The 3′ and 5′ flanking regions required for homologous recombination into the lactococcal chromosome were obtained by digestion of pUC-5′NOX (20) with *Eco*RI and *Nsp*V, which generated a 1.1-kb fragment containing the upstream and 5′ coding region of *nox-2*, and by digestion of pUC-3′NOX (20) with *Eco*RI and *Ssp*I, which generated a 1.0-kb fragment containing the downstream and 3′ coding region of *nox-2*. These two fragments were cloned into *Hin*cII-*Nar*I-digested pUC19 by using three-point ligation. The resulting plasmid contained the entire *nox-2* gene (the 5′ and 3′ ends were fused at the *Eco*RI site) and was designated pUC-NOX. The erythromycin resistance gene was isolated as a *Pst*I-*Acc*I fragment from pUC19Ery (43) and was blunted by using T4 polymerase. This erythromycin resistance cassette was cloned into the *Eco*RI site of pUC-NOX after the *Eco*RI sticky ends were blunted by using Klenow polymerase. The resulting plasmid, containing the erythromycin resistance gene in the same orientation as the *nox-2* gene, was transformed into competent *L. lactis* MG1363 cells, and erythromycin-resistant colonies were selected. In 15 of these colonies the organization of the chromosomal *nox-2* locus was analyzed by Southern blotting, and two colonies that contained the desired double crossover *nox-2*::*ery* gene disruption were selected. One of these mutant strains (designated NZ9020) was selected and used in this study.

Growth conditions. Strains were grown in a 2-liter fermentor (B. Braun Biostat MD) in chemically defined medium (34) containing glucose (10 $g \cdot liter^{-1}$) at 30°C and pH 6.5 or 5.5. For growth of the NOX^+ and NOX^- strains, the medium was supplemented with chloramphenicol (10 $mg \cdot liter^{-1}$) and erythromycin (5 $mg \cdot liter^{-1}$), respectively. For overproduction of NADH oxidase by the NOX^+ strain, nisin (5 $\mu g \cdot liter^{-1}$) was added to the medium when an optical density at 600 nm (OD_{600}) of 0.5 was reached, and cells were harvested in the mid-log growth phase (OD_{600}, 2.2). Anaerobiosis was attained by flushing sterile argon through the medium in the fermentor for 1 h before inoculation. Under aerobic conditions, dissolved oxygen was monitored with a polarographic oxygen electrode (Ingold). The electrode was calibrated to zero and 100% by bubbling sterile argon and air, respectively, through the medium. A specific air tension of 90% was maintained by automatic control of the airflow.

In vivo NMR experiments. Cells were harvested in the mid-log growth phase (OD_{600}, 2.2), centrifuged, washed twice, and suspended in 50 mM potassium phosphate (KP_i) buffer (pH 6.5, 5.5, or 4.5) to a protein concentration of approximately 13 $mg \cdot ml^{-1}$ (equivalent to 22 mg [dry weight] $\cdot ml^{-1}$), and the suspension was placed in a bioreactor (50 ml). Anaerobic conditions were established as described previously (32), but the thickness of the tubing was increased to 0.8 mm. For experiments under an O_2 atmosphere, a micro pO_2 electrode (Lazar Research Laboratories, Inc.) was included in the experimental setup described previously (32). To ensure an adequate level of oxygenation, an air lift system (37) with pure oxygen was used inside the NMR tube, and in addition, oxygen was continuously bubbled through the cell suspension in the bioreactor; the rate of circulation of the cell suspension between the fermentor and the NMR tube was 36 $ml \cdot min^{-1}$.

In vivo determination of NAD^+ and NADH by ^{13}C-NMR was carried out with cell suspensions grown in chemically defined medium without aspartate and asparagine and supplemented with nicotinic acid (5 $mg \cdot liter^{-1}$) specifically labeled on carbon 5 as described by Neves et al. (31). The NOX^+ strain was unable to grow in this medium.

After acquisition of an initial spectrum, [1-^{13}C]glucose or [6-^{13}C]glucose (20 mM) was supplied, and the time courses for glucose consumption, product formation, and buildup and decline of intracellular metabolite pools were monitored. The use of [6-^{13}C]glucose allowed monitoring of the resonances of intracellular glucose 6-phosphate (G6P) that otherwise were obscured by the intense resonances due to [1-^{13}C]glucose. Identical intracellular pools were observed for all metabolites other than G6P regardless of the position of the label in glucose. After glucose exhaustion and when no changes in the resonances due to end products and intracellular metabolites were observed, an aliquot of the cell suspension was passed through a French press; the resulting cell extract was incubated at 80°C for 10 min in a stoppered tube and cooled on ice, and cell debris and denatured macromolecules were removed by centrifugation. The supernatant, designated the NMR sample extract, was used for quantification of end products and minor metabolites.

Although the results of individual experiments are shown below, NMR experiments were performed at least twice for each type of experimental conditions and were highly reproducible. ^{13}C spectra were acquired with a Bruker DRX500 spectrometer at 30°C by using a quadruple-nucleus probe head (32). Carbon chemical shifts were referenced to the resonances of external methanol designated at 49.3 ppm.

Quantification of end products. Lactate, acetoin, acetate, 2,3-butanediol, and formate were quantified in NMR sample extracts by ^1H-NMR (32). The concentrations of minor products (e.g., pyruvate, ethanol, and diacetyl) and the concentrations of metabolites present at the end of the in vivo NMR experiments (phosphoenolpyruvate [PEP] and 3-phosphoglycerate [3-PGA]) in NMR sample extracts were determined by ^{13}C analysis as previously described (33).

Quantification of intracellular metabolites in living cells by ^{13}C-NMR. Due to the fast pulsing conditions used to acquire in vivo ^{13}C spectra, a direct correlation between concentrations and peak intensities could be established only by using correction factors. The correction factors for C-1 and C-6 of fructose 1,6-bisphosphate [Fru(1, 6)P_2] (0.73 ± 0.03) and for C-3 of 3-PGA and PEP (0.71 ± 0.01) were determined as described by Neves et al. (33). For C-6 of G6P, the correction factor (0.63 ± 0.04) was determined from spectra of an NMR sample extract to which G6P (30 mM) was added; the extract was circulated through the NMR tube at a rate similar to that used for suspensions of living cells. The quantitative kinetic data for intracellular metabolites were calculated from the areas of the corresponding resonances by using the correction factors and comparing the intensities with the intensity of the lactate resonance in the last spectrum of the sequence.

Metabolite concentrations were calculated by using a value of 2.9 $\mu l \cdot mg$ of $protein^{-1}$ for the intracellular volume (35). The concentration limit for detection of intracellular metabolites under the conditions used to acquire spectra of living cells (acquisition time, 30 s) was approximately 4 mM.

Enzyme activity measurements. All enzymes were assayed at 30°C by using freshly prepared cell extracts. The extracts were obtained by disruption of cell suspensions (prepared as described above for NMR experiments; OD_{600}, 2.2) in a French press (three passages, 120 MPa), followed by centrifugation at 30,000 × *g*. The protein concentration was determined by the method of Bradford (5). L-Lactate dehydrogenase (LDH) (EC 1.1.1.27) and pyruvate kinase (PK) (EC 2.7.1.40) activities were measured as described previously (15). Glyceraldehyde 3-phosphate dehydrogenase (Gra-3-P dehydrogenase) (EC 1.2.1.12) was assayed as described by Even et al. (13). 6-Phosphofructokinase (PFK) (EC 2.7.1.11) activity was measured by the method of Fordyce et al. (14).

To measure enolase activity, a modification of the assay described by Schäfer and Schönheit (38) was used; the 1-ml reaction mixtures contained 100 mM Tris-HCl buffer (pH 7.2), 5 mM $MgCl_2$, 5 mM ADP, 0.3 mM NADH, 10 U of PK (rabbit muscle), and 10 U of LDH (pig heart muscle), and 2-PGA (3 mM) was used to initiate the reaction.

NADH peroxidase activity was measured under anaerobic conditions by using a modification of the assay described by Zitzelsberger et al. (44). The 1-ml assay mixture contained 50 mM Tris-HCl (pH 7.8), 0.3 mM NADH, and 10 mM H_2O_2. SOD (EC 1.15.1.1) activity was measured by using the protocol of Beauchamp and Fridovich (2), in which a xanthine-xanthine oxidase system is used to generate O_2^- and nitroblue tetrazolium is used as an indicator. One unit of SOD activity was defined as the amount of SOD that resulted in 50% inhibition of the reduction of nitroblue tetrazolium. Total NADH oxidase activity (sum of H_2O-forming NADH oxidase, H_2O_2-forming NADH oxidase, and NADH peroxidase activities) was measured as described by Lopez de Felipe et al. (27). H_2O_2-forming NADH-dependent activity was determined by measuring the amount of H_2O_2 formed in 1-ml reaction mixtures containing 50 mM KP_i buffer (pH 7.0), 0.3 mM EDTA, and 0.3 mM NADH. The H_2O_2 formed was measured colorimetrically at 600 nm by the method described by Meiattini (30). The activity of H_2O-forming NADH oxidase was calculated from the difference between the total NADH oxidase activity and the H_2O_2-forming NADH-dependent activity and was corrected for NADH peroxidase activity.

Purification of NADH oxidase. *L. lactis* NOX^+ cells (34 g, wet weight) were harvested in the mid-log growth phase, washed twice with 5 mM KP_i buffer (pH 6.5), and suspended in the same buffer containing 0.5 mM phenylmethylsulfonyl fluoride, 2 μg of antipain per ml, and 2 μg of leupeptin per ml. A crude extract was prepared by passage through a French press and ultracentrifugation (5 h at 150,000 × *g*). The resulting supernatant was concentrated by ultrafiltration (Diaflo YM3; Amicon Corporation). Purification was performed by the method

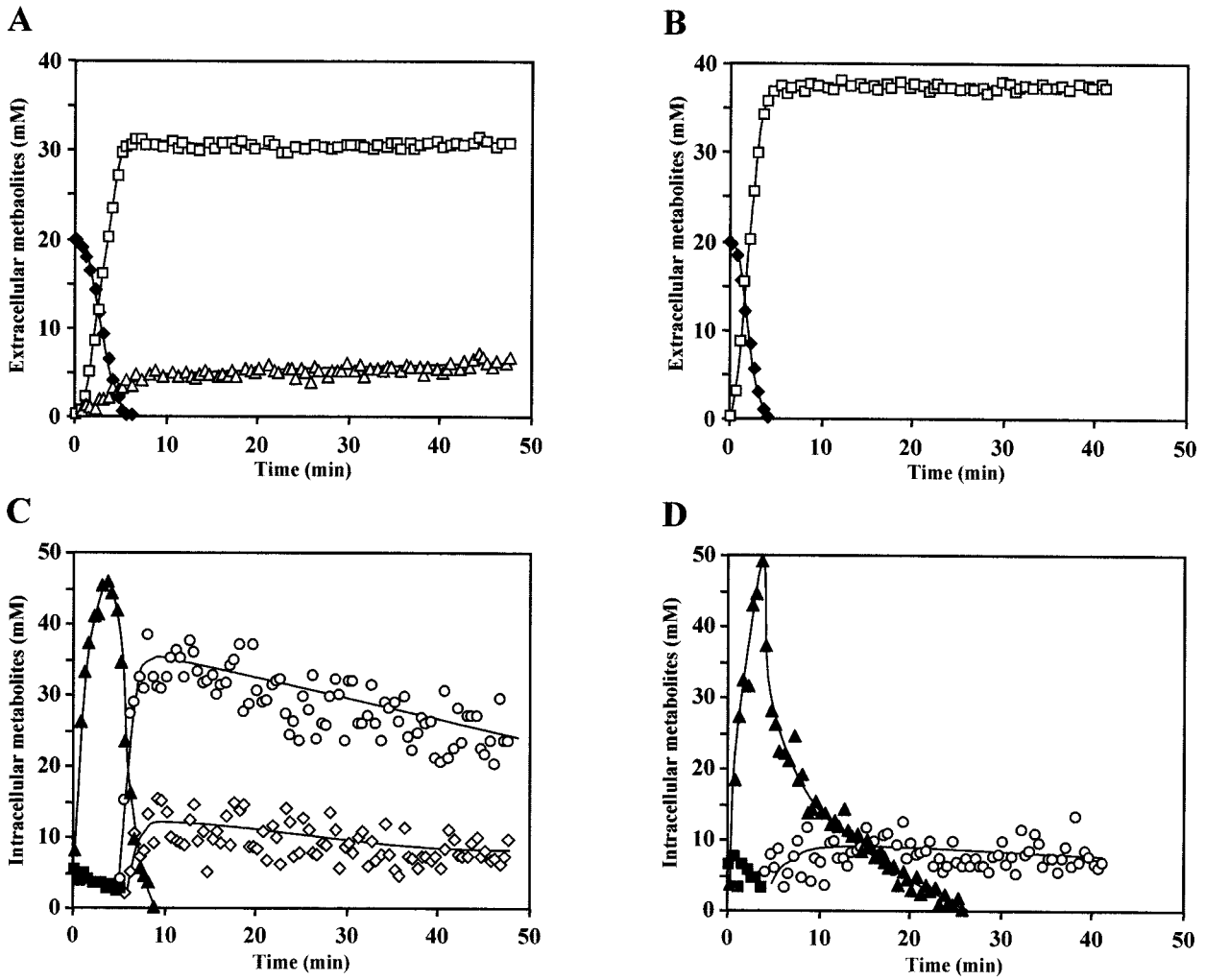

FIG. 1. Kinetics of [6-^{13}C]glucose consumption and product formation (A and B) and pools of intracellular metabolites (C and D) in MG1363 under an oxygen atmosphere (A and C) or under anaerobic conditions (B and D) as monitored by ^{13}C-NMR. For anaerobic studies, cells were grown in deaerated chemically defined medium, while aerobic growth was achieved by maintaining a constant air pressure of 80% in the bioreactor vessel. Symbols: ◆, glucose; □, lactate; △, acetate; ▲, Fru(1,6)P_2; ■, G6P; (○), 3-PGA; ◇, PEP.

described by Higuchi et al. (18) by using a first step consisting of precipitation with ammonium sulfate and four subsequent chromatographic steps (DEAE-Sepharose, Resource Q, phenyl-Sepharose HP, and Resource Q). All the purification steps were carried out in the presence of protease inhibitors. The enzyme preparation was determined to be pure by sodium dodecyl sulfate-polyacrylamide gel electrophoresis. The NADH oxidase activity assay described above was used to monitor the presence of the enzyme during the purification procedure. The protein concentration was determined from the A_{271} by using the molar extinction coefficient $\varepsilon_{271} = 69.8\ mM^{-1} \cdot cm^{-1}$, which was calculated from quantification of amino acid residues in a Pico · Tag amino acid analysis system after acid hydrolysis and derivatization with phenylisothiocyanate.

Determination of the affinity of NADH oxidase for oxygen. To determine the K_m of NADH oxidase for oxygen, oxymyoglobin was used as an oxygen probe (3). Oxymyoglobin was prepared from horse myoglobin as described by Jünemann et al. (25) and was diluted to a concentration of approximately 14.5 μM in 50 mM KP_i buffer (pH 7.0)–1 mM EDTA saturated with 1% (vol/vol) oxygen in argon. All other solutions used were made anaerobic by sparging with argon. A quartz cuvette was flushed with argon and filled with 2.5 ml of the oxymyoglobin solution, and NADH (1.2 mM) was added. The reaction was started by injecting the purified NADH oxidase (22.7 nM), and visible spectra were acquired sequentially. From the difference in the absorbance values at 580 and 562 nm and the dissociation constant for the reaction of myoglobin with oxygen (K_d = 1.2 μM), the mean concentration of free dissolved oxygen was determined. The rate of oxygen consumption was determined from the time dependency of the total oxygen concentration. Microsoft EXCEL Solver was used to determine the kinetic parameters (K_m and V_{max}) from the plots of rate of oxygen consumption versus oxygen concentration.

Chemicals. [1-^{13}C]glucose and [6-^{13}C]glucose (99% ^{13}C enrichment) were obtained from Campro Scientific (Veenendaal, The Netherlands) and ISOTEC (Miamisburg, Ohio), respectively. Horse heart myoglobin was obtained from Sigma Chemical Co. (St. Louis, Mo.). Chromatographic materials were supplied by Pharmacia Fine Chemicals (Uppsala, Sweden). All other chemicals were reagent grade.

RESULTS

Glucose metabolism by the wild-type strain: effect of oxygen. In vivo NMR was used to study glucose metabolism at pH 6.5 by nongrowing cell suspensions of *L. lactis* MG1363 under aerobic and anaerobic conditions. Figure 1 shows the kinetics of glucose consumption, end product formation (Fig. 1A and B), and evolution of intracellular metabolite pools (Fig. 1C and D) under aerobic (100% oxygen) and anaerobic conditions. In

TABLE 1. Comparison of enzyme specific activities in crude extracts of MG1363 cells grown under anaerobic and aerobic conditions[a]

Enzyme	Activity		Aerobic/anaerobic ratio
	Anaerobic conditions	Aerobic conditions	
PFK	1.01 ± 0.02	0.63 ± 0.00	0.62
PK	1.97 ± 0.17	1.44 ± 0.02	0.73
LDH	30.62 ± 0.61	16.92 ± 0.98	0.55
Gra-3-P dehydrogenase	29.68 ± 0.67	36.11 ± 2.68	1.22
Enolase	2.08 ± 0.07	1.76 ± 0.08	0.85
H_2O_2-forming NADH oxidase	0.01 ± 0.00	0.02 ± 0.00	2.00
H_2O-forming NADH oxidase	0.04 ± 0.00	0.15 ± 0.01	3.75
NADH peroxidase	0.02 ± 0.00	0.05 ± 0.00	2.50
Total NADH oxidase[b]	0.07 ± 0.01	0.22 ± 0.01	3.14
SOD	7.13 ± 0.25	7.84 ± 0.20	1.10

[a] Enzyme activities are expressed in micromoles per minute per milligram of protein and are means ± standard deviations ($n \geq 4$).
[b] Total NADH oxidase activity is the sum of the H_2O-forming NADH oxidase, H_2O_2-forming NADH oxidase, and NADH peroxidase activities as measured by the method of Lopez de Felipe et al. (27).

the absence of oxygen the glucose consumption rate (0.41 ± 0.01 $\mu mol \cdot min^{-1} \cdot mg$ of $protein^{-1}$) was 1.6-fold higher than the glucose consumption rate under aerobic conditions (0.25 ± 0.03 $\mu mol \cdot min^{-1} \cdot mg$ of $protein^{-1}$).

With respect to intracellular metabolites, the G6P pool was maximal within the first few seconds after glucose addition and decreased to undetectable levels parallel with the decrease in the glucose level. Meanwhile, the concentration of Fru(1,6)P_2 reached maxima of 48.8 ± 0.4 mM (anaerobic conditions) and 45.5 ± 0.2 mM (aerobic conditions). The decline in the Fru(1,6)P_2 level was significantly steeper under aerobic conditions, under which it was accompanied by increases in the 3-PGA and PEP concentrations, which reached maximal levels of 33 ± 3 and 13 ± 2 mM, respectively. Under anaerobic conditions, the concentrations of these compounds were lower, 8 ± 2 and 3 ± 1 mM, respectively. The low PEP concentration (close to the in vivo detection limit) hampered reliable quantification in vivo; therefore, the concentration of PEP was determined by using NMR sample extracts.

Under aerobic conditions, lactate (final concentration, 31.4 ± 1.1 mM) was the major product, but about 16% of the carbon flux was channeled towards the production of acetate (6.7 ± 0.7 mM). Under anaerobic conditions, glucose was almost completely metabolized to lactate (37.4 ± 0.3 mM), and acetate (0.5 ± 0.1 mM) accounted only for 1.3% of the carbon from glucose. Other minor products that were detected were ethanol and formate under anaerobic conditions, acetoin under aerobic conditions, and 2,3-butanediol under both conditions.

To rationalize the metabolic data, relevant enzymatic activities were measured in cell extracts of cultures grown under aerobic or anaerobic conditions (Table 1). The activities of the glycolytic enzymes encoded by the *las* operon, PFK, PK, and LDH, as well as the activity of enolase, decreased significantly in cells grown under aerobic conditions, and the change in LDH activity was especially noticeable; in contrast, the activity of Gra-3-P dehydrogenase increased slightly. The possibility of a direct effect of oxygen on the enzyme activities could be eliminated since the same results were obtained regardless of whether aerobic or anaerobic conditions were used for the assay (data not shown). NADH peroxidase activity, H_2O_2-forming activity dependent on NADH, and H_2O-forming NADH oxidase activity were induced 2.5-, 2- and 3.8-fold, respectively, in cells grown under aerobic conditions, whereas SOD activity was not affected.

Characterization of glucose metabolism in a strain overproducing NADH oxidase. The total NADH oxidase activity in cultures of the NOX^+ strain grown under aerobic conditions without nisin induction was similar to that of strain MG1363 (about 0.22 $\mu mol \cdot min^{-1} \cdot mg$ of $protein^{-1}$). Induction with 5 μg of nisin per liter resulted in an 80-fold increase in this enzymatic activity (17 $\mu mol \cdot min^{-1} \cdot mg$ of $protein^{-1}$). Figure 2 shows a selection of ^{13}C spectra acquired during the metabolism of 20 mM [6-^{13}C]glucose by a cell suspension of the NOX^+ strain under an oxygen-saturated atmosphere. The concentrations of the end products acetoin, acetate, and lactate were monitored as a function of time along with the concentrations of the intracellular metabolites [1-^{13}C]Fru(1,6)P_2, [6-^{13}C]Fru(1,6)P_2, G6P, 3-PGA, and PEP during the metabolism of glucose (20 mM) by cell suspensions of the NOX^+ strain under an oxygen-saturated atmosphere (Fig. 3A and C). Glucose metabolism was rerouted towards the production of acetoin (10.4 ± 0.3 mM) and acetate (12.1 ± 0.7 mM), as well as trace amounts (0.3 ± 0.1 mM) of diacetyl (as determined by ^{13}C-NMR analysis of NMR sample extracts). This metabolic shift represented a 60-fold increase in the flux through α-acetolactate synthase (from less than 0.01 in strain MG1363 to 0.60 in the NOX^+ strain) and a 2-fold increase in the flux through pyruvate dehydrogenase; on the other hand, lactate (2.3 ± 0.5 mM) accounted for only 6% of the carbon in glucose. Once glucose was added, the G6P and Fru(1,6)P_2 concentrations increased to 7 ± 1 and 29 ± 1 mM (averages of four experiments), respectively; the Fru(1,6)P_2 concentration was significantly lower than the maximal Fru(1,6)P_2 concentration reached in strain MG1363 under the same conditions (Fig. 1C). At the onset of glucose exhaustion, the 3-PGA and PEP concentrations increased, leveling off at 36 ± 3 and 15 ± 3 mM, respectively.

In separate experiments, the intracellular P_i and nucleoside triphosphate (NTP) levels, as well as the evolution of the intracellular pH, were monitored in vivo by ^{31}P-NMR (Fig. 3E). The concentration of NTP increased from undetectable levels to a maximum of 8.8 ± 0.5 mM and then dropped to undetectable levels soon after glucose exhaustion (at ~19 min). Concomitant with NTP depletion, a sudden rise in the intracellular P_i concentration from 5 mM to about 22 mM was observed, followed by a gradual increase to the initial level (about 38 mM). Addition of glucose caused a sudden increase in the intracellular pH (1.08 pH units), which also returned slowly to its initial value once glucose was depleted.

In the absence of oxygen, the glucose metabolism of the NOX^+ strain resembled that of strain MG1363, with 93% of the carbon being converted to lactate (Fig. 3B). The profiles of intracellular metabolites were also identical, although a slightly higher PEP concentration (6 ± 2 mM) was measured in the NOX^+ strain. The total NADH oxidase activity measured in cell extracts of the NOX^+ strain grown under anaerobic conditions was 16.5 $\mu mol \cdot min^{-1} \cdot mg$ of $protein^{-1}$, which was 235-fold higher than the total NADH oxidase activity found for

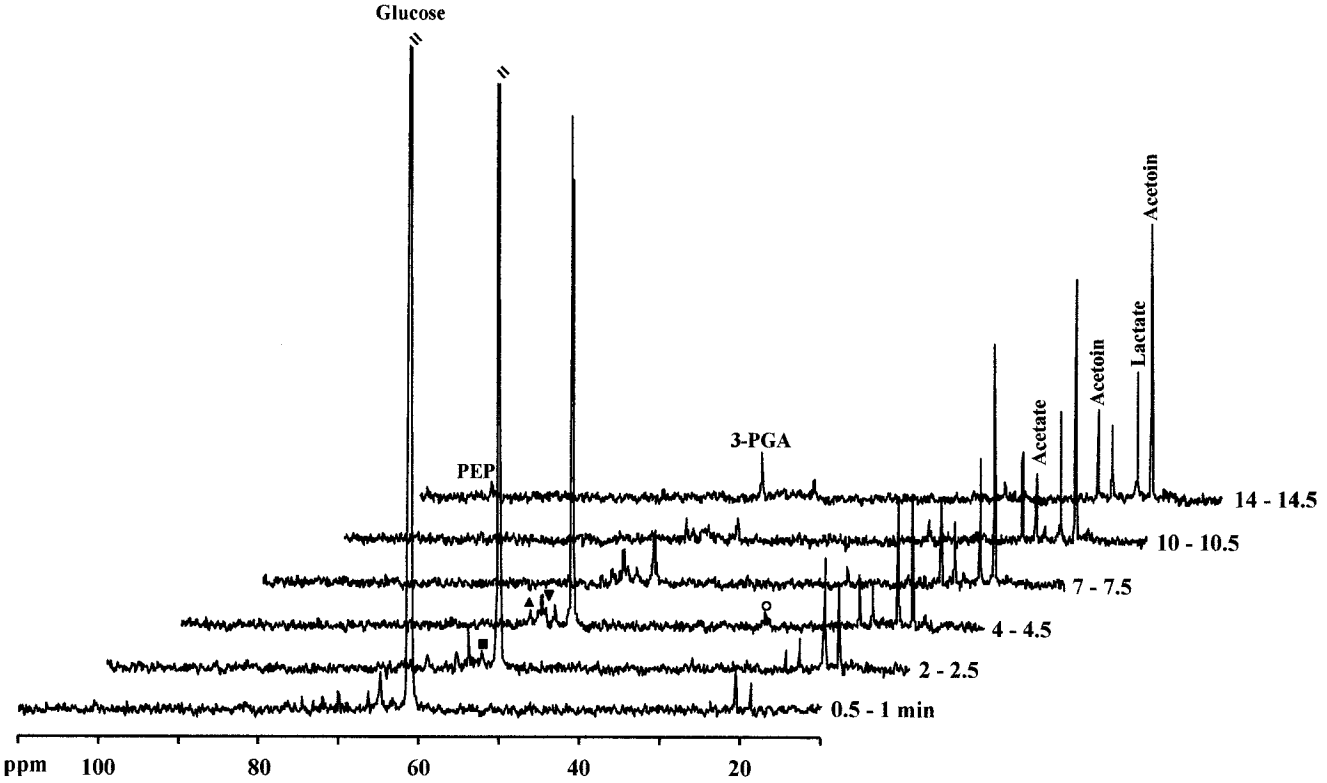

FIG. 2. Series of ^{13}C spectra during glucose metabolism by the NOX^+ strain. Each spectrum represents 30 s of acquisition. Glucose was added at time zero, and each spectrum was acquired during the indicated interval and was processed with 5-Hz line broadening. Symbols: ▲, [1-^{13}C]Fru(1,6)P_2; ▼, [6-^{13}C]Fru(1,6)P_2; ■, G6P; ○, aspartate.

strain MG1363 (0.07 $\mu mol \cdot min^{-1} \cdot mg$ of $protein^{-1}$) grown under the same conditions.

Characterization of glucose metabolism in a strain deficient in NADH oxidase. Glucose metabolism in a strain carrying a deletion of the lactococcal *nox-2* gene was also examined by ^{13}C-NMR in vivo (Fig. 4). A residual total NADH oxidase activity of 0.025 $\mu mol \cdot min^{-1} \cdot mg$ of $protein^{-1}$ was determined in the cells, probably due to H_2O_2-forming activity (NADH dependent) coupled with peroxidase activity. Also, a contribution by H_2O-forming NADH oxidases other than that encoded by the *nox-2* gene cannot be ruled out. Under anaerobic conditions, this strain produced lactate (37.2 ± 1.2 mM) and trace amounts of acetate, ethanol, 2,3-butanediol, and formate during metabolism of 20 mM glucose (Fig. 4). Under aerobic conditions, the amount of acetate produced was significantly higher (3.7 ± 0.6 mM), corresponding to 9% of the carbon flux. The Fru(1,6)P_2 concentration reached maximal levels of 45.5 ± 0.7 mM (anaerobic conditions) and 38.7 ± 0.7 mM (aerobic conditions). In the presence of O_2, the pattern of Fru(1,6)P_2 consumption was similar to that exhibited by strain MG1363, but under anaerobic conditions the decline in the Fru(1,6)P_2 concentration was considerably slower, and the levels of 3-PGA and PEP were below the detection limits of the in vivo NMR procedure. For the corresponding NMR sample extracts, a value of 3 mM was calculated for the intracellular concentration of 3-PGA, but PEP was not detected. Under an oxygen atmosphere the 3-PGA concentration reached a maximum of 25 ± 3 mM; PEP could not be detected in vivo, but a concentration of 3.9 ± 0.3 mM was observed in vitro. These results show that the presence of oxygen had a significant impact on intermediates and end products of glucose metabolism, even in cells with very low total NADH oxidase activity. Table 2 summarizes the data for the maximal values determined for intracellular metabolites in the three strains examined under aerobic and anaerobic conditions. Data for the glucose consumption rate and total NADH oxidase activity are also presented.

The crucial role of pyridine nucleotides in the metabolism of *L. lactis* means that they must be studied in a noninvasive manner. The evolution of NAD^+ and NADH concentrations in the NOX^- strain during the consumption of glucose (80 mM) under anaerobic conditions was monitored in vivo with a time resolution of 2.2 min (Fig. 4C). Before glucose addition (starved cells) the level of NAD^+ was 3.3 mM, and it remained constant while glucose was available. At the onset of glucose depletion the NAD^+ concentration dropped abruptly to 1.2 mM concomitant with a steep decline in the Fru(1,6)P_2 concentration. On the other hand, the level of NADH was below the detection limit of the in vivo NMR technique (0.5 mM) and increased to circa 1.8 mM once glucose was exhausted. After this, the levels of Fru(1,6)P_2 (8 mM), NAD^+ (1.2 mM), and NADH (1.8 mM) remained unchanged (Fig. 4C).

Effect of pH on the pattern of intracellular metabolites and end products. A comparison of the end products resulting from the metabolism of glucose by the MG1363 and NOX^+ strains at different pH values (pH 6.5, 5.5, and 4.5) under

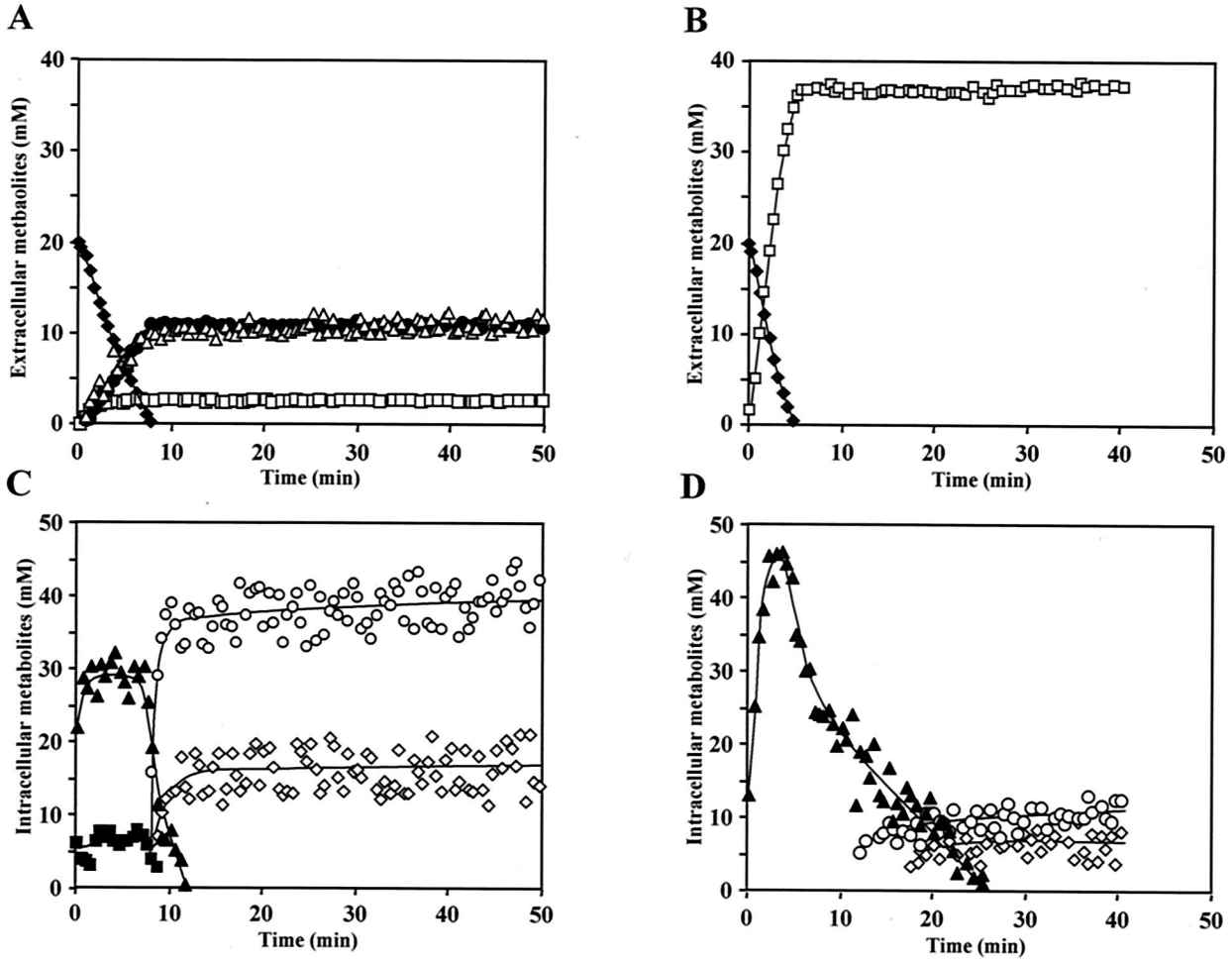

FIG. 3. (A to D) Kinetics of [6-^{13}C]glucose consumption and product formation (A and B) and pools of intracellular metabolites (C and D) in the NOX$^+$ strain under an oxygen atmosphere (A and C) or under anaerobic conditions (B and D) as determined by ^{13}C-NMR. (E) Biochemical parameters determined by ^{31}P-NMR during metabolism of glucose in the NOX$^+$ strain under aerobic conditions. The shaded area indicates glucose availability. Symbols: ◆, glucose; □, lactate; △, acetate; ●, acetoin; ▲, Fru(1,6)P_2; ■, G6P; ○, 3-PGA; ◇, PEP; ∗, NTP; ▽, P_i; ▼, intracellular pH.

aerobic conditions is shown in Table 3; the corresponding data for maximal levels of phosphorylated metabolites are shown in Table 4. The glucose metabolism of strain MG1363 at pH 5.5 and 6.5 was also investigated under anaerobic conditions; no significant pH-dependent changes in the pattern of end products were found (data not shown), although decreased maximal levels of Fru(1,6)P_2 (38 mM), 3-PGA (6 mM), and PEP (<0.5 mM) were observed at pH 5.5.

In strain MG1363, the concentration of acetoin increased from 0.13 to 2.65 mM when the pH was decreased from 6.5 to 5.5, but diacetyl production was not detected. This flavor compound, however, was produced by the NOX$^+$ strain, especially at the lower pH values. In strain MG1363, the stimulation of acetoin production at a lower pH was accompanied by a reduction in lactate production, whereas the most pronounced effect in the NOX$^+$ strain was the decrease in acetate production. Therefore, lowering the pH to 5.5 under aerobic conditions influenced the distribution of the pyruvate flux via LDH and α-acetolactate synthase in strain MG1363. In contrast, the pH-induced decrease in acetate production by the NOX$^+$ strain reflected the pH dependence of α-acetolactate synthase, which becomes more competitive than pyruvate dehydrogenase at lower pH values (41). The lower NADH oxidase activity in the NOX$^+$ strain at pH values below 6.5 is likely to be due to inactivation of the enzyme by diacetyl (23).

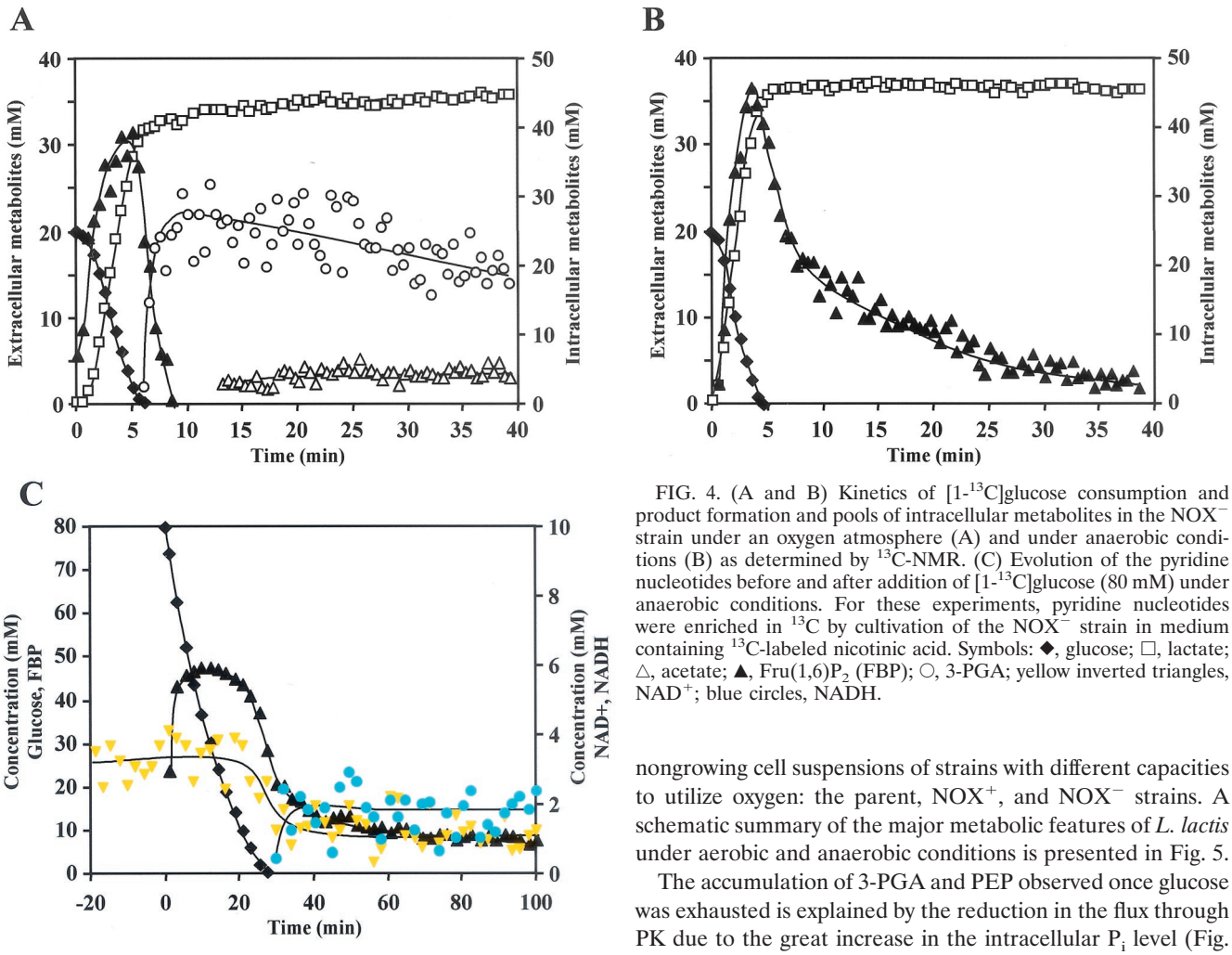

FIG. 4. (A and B) Kinetics of [1-^{13}C]glucose consumption and product formation and pools of intracellular metabolites in the NOX$^-$ strain under an oxygen atmosphere (A) and under anaerobic conditions (B) as determined by ^{13}C-NMR. (C) Evolution of the pyridine nucleotides before and after addition of [1-^{13}C]glucose (80 mM) under anaerobic conditions. For these experiments, pyridine nucleotides were enriched in ^{13}C by cultivation of the NOX$^-$ strain in medium containing ^{13}C-labeled nicotinic acid. Symbols: ◆, glucose; □, lactate; △, acetate; ▲, Fru(1,6)P_2 (FBP); ○, 3-PGA; yellow inverted triangles, NAD$^+$; blue circles, NADH.

A remarkable reduction in the intracellular metabolite concentrations was observed in strain MG1363 when the pH was decreased from 6.5 to 5.5 (Table 4); for example, the Fru(1,6)P_2 and 3-PGA concentrations decreased approximately twofold, and the reduction in the PEP concentration was even greater (threefold). Interestingly, in the NOX$^+$ strain, the Fru(1,6)P_2 concentration was affected only slightly, but the extents of reduction in the 3-PGA and PEP concentrations were as great as the extents of reduction for strain MG1363.

NADH oxidase affinity for oxygen. To explain the metabolic behavior of the NOX$^+$ strain in the presence of oxygen, it was deemed important to know the kinetic parameters of the overproduced enzyme, H_2O-forming NADH oxidase, for its substrates. The K_m of *S. mutans* NADH oxidase for NADH was reported to be approximately 25 μM (18), but the affinity for oxygen is unknown. Therefore, the enzyme was purified, and the affinity for oxygen was determined in this study. A K_m of 2 μM for O_2 was found. To our knowledge, this is the first report of the oxygen affinity of any NADH oxidase.

DISCUSSION

To obtain a reliable picture of the oxygen-induced changes in glucose metabolism, we used in vivo ^{13}C-NMR analysis of nongrowing cell suspensions of strains with different capacities to utilize oxygen: the parent, NOX$^+$, and NOX$^-$ strains. A schematic summary of the major metabolic features of *L. lactis* under aerobic and anaerobic conditions is presented in Fig. 5.

The accumulation of 3-PGA and PEP observed once glucose was exhausted is explained by the reduction in the flux through PK due to the great increase in the intracellular P_i level (Fig. 3E) (32, 29); the preponderant contribution of P_i to PK inhibition is further supported by the observation that the great increase in 3-PGA and PEP levels occurred when the levels of Fru(1,6)P_2 and G6P (two activators of PK) were still high (a few millimolar) and above the K_a values reported for activation of the pure enzyme (42). Therefore, before glucose was added, PK was virtually inoperative. As a consequence of this bottleneck, in the initial stage of glucose metabolism the oxidation of NADH formed at the level of Gra-3-P dehydrogenase was restricted, leading to inhibition of this enzyme. Therefore, Fru(1,6)P_2 accumulated until a steady-state concentration was attained, whose magnitude was consistently lower under aerobic conditions (Table 2). The lower concentration of Fru(1,6)P_2 when oxygen was present reflected the involvement of the NADH oxidase activity in the initial stage of glucose metabolism, assisting LDH in the oxidation of NADH produced at the level of Gra-3-P dehydrogenase and allowing a higher flux through this redox step. This explanation is supported by the reduced Fru(1,6)P_2 level in the NOX$^+$ strain and by the observation that in the absence of oxygen, the three strains accumulated Fru(1,6)P_2 to similar extents. However, the high levels of Fru(1,6)P_2 accumulating in the NOX$^+$ strain despite the high NADH oxidase activity (comparable to the activity of LDH) appear not to fit this interpretation and sug-

TABLE 2. NADH oxidase activity, glucose consumption rate, and maximal concentrations of glycolytic intermediates in the wild-type, NOX^+, and NOX^- strains grown in the presence of argon or an O_2 atmosphere at pH 6.5

Strain	Conditions	Total NADH oxidase activity ($\mu mol \cdot min^{-1} \cdot mg$ of protein^{-1})[a]	Glucose consumption rate ($\mu mol \cdot min^{-1} \cdot mg$ of protein^{-1})	Concn (mM) of:			
				G6P	Fru(1,6)P_2	3-PGA	PEP
MG1363	Argon	0.07 ± 0.01	0.41 ± 0.01	8 ± 2	49 ± 0.4	8 ± 2	3 ± 1
	O_2	0.22 ± 0.01	0.25 ± 0.03	5 ± 1	46 ± 0.2	33 ± 3	13 ± 2
NOX^+	Argon	16.5 ± 0.23	0.35 ± 0.02	—[b]	46 ± 0.6	10 ± 2	6 ± 2
	O_2	17.0 ± 0.50	0.21 ± 0.02	7 ± 1	29 ± 1	36 ± 3	15 ± 3
NOX^-	Argon	0.03 ± 0.00	0.37 ± 0.03	—	46 ± 0.7	3 ± 0.4	ND[c]
	O_2	0.03 ± 0.00	0.23 ± 0.04	—	39 ± 0.7	25 ± 3	4 ± 0.3

[a] Total NADH oxidase activity (sum of H_2O-forming NADH oxidase activity, H_2O_2-forming activity dependent on NADH, and NADH peroxidase activity) was determined by the method of Lopez de Felipe et al. (27). All determinations of NADH oxidase activity were done at least twice with two extracts obtained from different cultures.
[b] —, not determined.
[c] ND, not detected.

gest that the reason for Fru(1,6)P_2 accumulation could be more complex.

Inhibition of PK alone does not explain the oxygen-dependent differences observed in the 3-PGA and PEP levels. Upon glucose depletion the levels of 3-PGA and PEP started to increase immediately, and therefore, they were derived from the residual high concentration of Fru(1,6)P_2. At this stage, consumption of the Fru(1,6)P_2 could proceed only at a rate determined by the rate of regeneration of NADH formed in the step catalyzed by Gra-3-P dehydrogenase. Under an oxygen atmosphere, the activity of NADH-utilizing enzymes allowed fast regeneration of this coenzyme, and therefore, the rate of consumption of Fru(1,6)P_2 was also high. The rapid depletion of Fru(1,6)P_2, combined with PK inhibition, led to the higher 3-PGA and PEP levels observed under aerobic conditions. In accordance with this interpretation, the relative sizes of the 3-PGA and PEP pools accumulating under aerobic conditions in the three strains examined ($NOX^+ \geq$ MG1363 > NOX^-) correlated with the relative levels of the total NADH oxidase activity.

When NADH oxidases were inoperative (anaerobic conditions), the level of Fru(1,6)P_2 decreased slowly once glucose was exhausted, and the concentrations of PEP and 3-PGA reached levels much lower than those observed under aerobic conditions; these typical features associated with anaerobic conditions were strongly accentuated in the NOX^- strain. In fact, the Fru(1,6)P_2 concentration was still about 8 mM 1 h after the glucose was exhausted (Fig. 4C); on the other hand, the level of NAD^+, which dropped noticeably at the onset of glucose depletion, did not increase to the initial value, as observed in strain MG1363 (31). Moreover, PEP and 3-PGA were undetectable. If the train of thought described above is followed, these features reflect the extreme limitation of this strain in terms of its ability to oxidize NADH formed during the metabolism of residual Fru(1,6)P_2; the high level of NADH (up to 2 mM) could inhibit Gra-3-P dehydrogenase, shifting the major metabolic bottleneck from PK to this dehydrogenase. As a consequence, in this strain, Fru(1,6)P_2 was the major residual metabolite instead of 3-PGA or PEP.

Surprisingly, the dynamics of intracellular metabolite concentrations in the NOX^- strain when it was metabolizing glucose in the presence of oxygen were similar to those of strain MG1363, particularly with respect to the rapid depletion of Fru(1,6)P_2 once glucose was exhausted. This behavior is explained by an NADH oxidase activity (Table 2) associated with NADH-utilizing enzymes other than the H_2O-forming NADH oxidase (*noxE* gene, designated *nox-2* here), which appears to contribute significantly to the regeneration of NAD^+ in this strain. In fact, several NADH oxidases and dehydrogenases (*noxA*, *noxB*, *noxC*, *noxD*, and *noxE* gene products) have been identified in the recently annotated genome sequence of *L. lactis* IL-1403 (4). This is also the rational basis for the production of acetate (9% of the total products) by the NOX^- strain under aerobic conditions, in contrast to the equivalent *S. mutans* mutant that produces vestigial amounts of acetate (19).

With regard to the profile of end products, the different levels of NADH oxidase in the three strains examined led to remarkable changes when oxygen was present. The data obtained with the NOX^+ strain confirm that overexpression of the *nox* gene is a viable strategy to achieve remarkable en-

TABLE 3. Concentrations of end products and glucose consumption rate in the MG1363 and NOX^+ strains at different pH values under aerobic conditions[a]

Strain	pH	Glucose consumption rate ($\mu mol \cdot min^{-1} \cdot mg$ of protein^{-1})	Concn (mM) of:				
			Lactate	Acetate	Acetoin	2,3-Butanediol	Diacetyl
MG1363	6.5	0.25 ± 0.03	31.4 ± 1.1	6.7 ± 0.7	0.1 ± 0.0	0.1 ± 0.0	ND[b]
	5.5	0.24 ± 0.02	25.4 ± 0.9	7.3 ± 0.6	2.5 ± 0.2	0.1 ± 0.0	ND
NOX^+	6.5	0.21 ± 0.01	2.3 ± 0.5	12.1 ± 0.7	10.4 ± 0.3	0.1 ± 0.0	0.3 ± 0.1
	5.5	0.17 ± 0.02	2.6 ± 0.3	7.3 ± 0.5	13.4 ± 0.1	0.1 ± 0.0	0.8 ± 0.0
	4.5	0.13 ± 0.02	1.9 ± 0.2	5.9 ± 0.3	11.6 ± 0.2	ND	1.6 ± 0.3

[a] The initial glucose concentration was 20 mM. All determinations were done at least twice with two extracts obtained from independent cultures.
[b] ND, not detected.

TABLE 4. Maximal concentrations of the glycolytic intermediates and NADH oxidase activity in the MG1363 and NOX$^+$ strains at different pH values under aerobic conditions

Strain	pH	Concn (mM) of:			NADH oxidase activity (μmol · min^{-1} · mg of protein^{-1})
		Fru(1,6)p$_2$	3-PGA	PEP	
MG1363	6.5	46 ± 0.2	33 ± 3	13 ± 2	0.15
	5.5	22 ± 1	14 ± 2	4 ± 0.5	0.11
NOX$^+$	6.5	29 ± 1	36 ± 3	15 ± 3	17.0
	5.5	23 ± 2	18 ± 3	5 ± 0.4	13.7
	4.5	23 ± 2	14 ± 3	4 ± 1	12.8

hancement in the carbon flux through α-acetolactate synthase (27); more importantly, when this strategy was combined with low-pH fermentation conditions, high levels of diacetyl were formed (Table 3).

The high NADH oxidase activity in the NOX$^+$ strain resulted in a shift of the major NADH oxidation site from LDH to NADH oxidase. The latter enzyme competed favorably with LDH due to its high (engineered) activity combined with its high affinity for its substrates (K_m of 25 μM for NADH [18] and K_m of 2 μM for O_2 [this study]). LDH has K_m values of 100 μM and 2 mM for NADH and pyruvate, respectively (9). In strain MG1363, the oxygen-induced rerouting of pyruvate away from lactate was not efficiently accomplished because the low expression levels of NADH oxidase were insufficient to compete with the much higher LDH activity.

Several workers have proposed that glycolysis is controlled primarily at the level of Gra-3-P dehydrogenase by the redox charge (15, 24, 32). Based on this model, one would expect that enhanced levels of NADH oxidase would result in enhancement of the flux through Gra-3-P dehydrogenase. However, the results presented here show that the glycolytic flux was not affected in response to the different levels of NADH oxidase activity. In particular, the observation that the glycolytic flux under aerobic conditions was not higher in the strain with huge overexpression of the *nox* gene (the NOX$^+$ strain) suggests that glycolytic flux is not primarily determined by the level of NADH in the cell.

Also, the general decrease in the glycolytic flux observed at saturating concentrations of oxygen cannot be explained on the basis of the expected lower redox charge that would enhance the flux through Gra-3-P dehydrogenase, but the toxicity associated with a high rate of oxygen consumption should not be ignored. The levels of PFK, PK, and primarily LDH were lower in cells grown under aerobic conditions (Table 1), but the

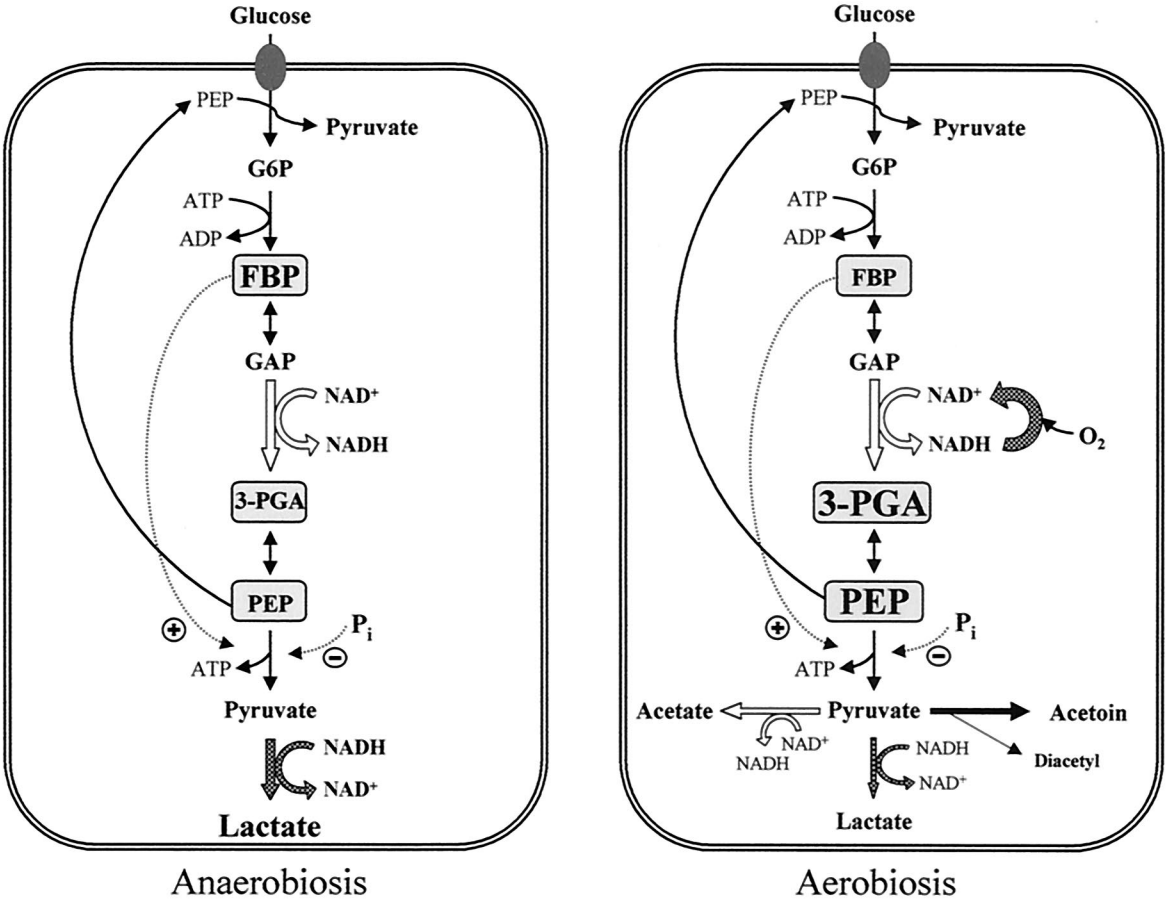

FIG. 5. Schematic representation of glucose metabolism under aerobic and anaerobic conditions in *L. lactis*. Major regulation sites described in the text are highlighted. The different sizes of the letters used for intracellular compounds reflect the different concentrations. FBP, fructose bisphosphate; GAP, glyceraldehyde 3-phosphate.

activities of these enzymes are still greater than the observed glycolytic flux (the ratios of enzymatic activity to flux through the enzyme were 2.5, 5.7, and 68, respectively). Curiously, the decrease in the level of PFK (40%) was identical to the decrease in the glycolytic flux. Moreover, a recent study showed that a twofold reduction in PFK activity in *L. lactis* resulted in a reduction of approximately 40% in the glycolytic flux (1). Therefore, the explanation for the negative effect exerted by oxygen on the glycolytic flux is likely to lie in part in the depressed activity of PFK.

At this stage it should be pointed out that in a previous study of *L. lactis* MG5267 grown under semianaerobic conditions, stimulation of glucose consumption when an oxygen atmosphere was established was observed (32); this apparent discrepancy shows that the level of oxygen during growth notably affected the cell metabolic machinery through different effects on gene expression. In accordance with this, Jensen et al. recently described the impact of oxygen on the level of enzymes downstream of the pyruvate branch point (24). Induction of responses to cope with oxygen toxicity was also detected in our studies; the H_2O_2-forming NADH-dependent activity and the activity of NADH peroxidase were enhanced during growth in the presence of oxygen (Table 1). Remarkably, resting MG1363 cells grown under strictly anaerobic conditions were unable to use glucose when they were exposed to saturating concentrations of oxygen (A. R. Neves, A. Ramos, and H. Santos, unpublished data), a result that shows that there is an urgent need for adaptation strategies in this bacterium.

In conclusion, the key role of NADH oxidases in the dynamics of intracellular metabolites and in the redirection of carbon fluxes was demonstrated in this study. Our efforts are now directed toward the development of a reliable mathematical model that will assist in the identification of genuine bottlenecks in cell metabolism.

ACKNOWLEDGMENTS

This work was supported by contracts BIO4CT-96-0498 and QKL1-CT-2000-01376 of the Commission of the European Communities and by Fundação para a Ciência e Tecnologia (FCT), Portugal, contract PRAXIS/P/BIA/11072/1998. A. R. Neves, H. Costa, and A. Ramos acknowledge research fellowships provided by FCT.

C. Maycock and R. Ventura are acknowledged for synthesis of labeled nicotinic acid.

REFERENCES

1. **Andersen, H. W., C. Solem, K. Hammer, and P. R. Jensen.** 2001. Twofold reduction of phosphofructokinase activity in *Lactococcus lactis* results in strong decreases in growth rate and in glycolytic flux. J. Bacteriol. **183:**3458–3467.
2. **Beauchamp, C., and I. Fridovich.** 1971. Superoxide dismutase: improved assays and an assay applicable to acrylamide gels. Anal. Biochem. **44:**276–287.
3. **Bergersen, F. J., and G. L. Turner.** 1979. Systems utilizing oxygenated leghemoglobin and myoglobin as sources of free dissolved O_2 at low concentrations for experiments with bacteria. Anal. Biochem. **96:**165–174.
4. **Bolotin, A., P. Wincker, S. Mauger, O. Jaillon, K. Malarme, J. Weissenbach, S. D. Ehrlich, and A. Sorokin.** 2001. The complete genome sequence of lactic acid bacterium *Lactococcus lactis* ssp. *lactis* IL1403. Genome Res. **11:**731–753.
5. **Bradford, M. M.** 1976. A rapid and sensitive method for the quantitation of microgram quantities of protein utilizing the principle of protein-dye binding. Anal. Biochem. **72:**248–254.
6. **Chen, R., and J. E. Bailey.** 1993. Observations of aerobic, growing *Escherichia coli* using an on-line nuclear magnetic resonance spectroscopy system. Biotechnol. Bioeng. **42:**215–221.
7. **Cogan, J. F., D. Walsh, and S. Condon.** 1989. Impact of aeration on the metabolic end products formed from glucose and galactose by *Streptococcus lactis*. J. Appl. Bacteriol. **66:**77–84.
8. **Condon, S.** 1987. Responses of lactic acid bacteria to oxygen. FEMS Microbiol. Rev. **46:**269–280.
9. **Crow, V. L., and G. G. Pritchard.** 1977. Fructose 1,6-diphosphate-activated L-lactate dehydrogenase from *Streptococcus lactis*: kinetic properties and factors affecting activation. J. Bacteriol. **131:**82–91.
10. **Davies, S. E., and K. M. Brindle.** 1992. Effects of overexpression of phosphofructokinase on glycolysis in the yeast *Saccharomyces cerevisiae*. Biochemistry **31:**4729–4735.
11. **de Graaf, A. A., K. Striegel, R. M. Wittig, B. Laufer, G. Schmitz, W. Wiechert, G. A. Sprenger, and H. Sahm.** 1999. Metabolic state of *Zymomonas mobilis* in glucose-, fructose-, and xylose-fed continuous cultures as analysed by ^{13}C- and ^{31}P-NMR spectroscopy. Arch. Microbiol. **171:**371–385.
12. **de Ruyter, P. G., O. P. Kuipers, M. M. Beerthuyzen, I. van Alen-Boerrigter, and W. M. de Vos.** 1996. Functional analysis of promoters in the nisin gene cluster of *Lactococcus lactis*. J. Bacteriol. **178:**3434–3439.
13. **Even, S., C. Garrigues, P. Loubiere, N. D. Lindley, and M. Cocaign-Bousquet.** 1999. Pyruvate metabolism in *Lactococcus lactis* is dependent upon glyceraldehyde-3-phosphate dehydrogenase activity. Metab. Eng. **1:**198–205.
14. **Fordyce, A. M., C. H. Moore, and G. G. Pritchard.** 1982. Phosphofructokinase from *Streptococcus lactis*. Methods Enzymol. **90:**77–82.
15. **Garrigues, C., P. Loubiere, N. D. Lindley, and M. Cocaign-Bousquet.** 1997. Control of the shift from homolactic acid to mixed-acid fermentation in *Lactococcus lactis*: predominant role of the NADH/NAD^+ ratio. J. Bacteriol. **179:**5282–5287.
16. **Gasson, M. J., K. Benson, S. Swindel, and H. Griffin.** 1996. Metabolic engineering of the *Lactococcus lactis* diacetyl pathway. Lait **76:**33–40.
17. **Hansson, L., and M. H. Häggstrom.** 1984. Effects of growth conditions on the activities of superoxide dismutase and NADH-oxidase/NADH-peroxidase in *Streptococcus lactis*. Curr. Microbiol. **10:**345–351.
18. **Higuchi, M., M. Shimada, Y. Yamamoto, T. Hayashi, T. Koga, and Y. Kamio.** 1993. Identification of two distinct NADH oxidases corresponding to H_2O_2-forming oxidase and H_2O-forming oxidase induced in *Streptococcus mutans*. J. Gen. Microbiol. **139:**2343–2351.
19. **Higuchi, M., Y. Yamamoto, L. B. Poole, M. Shimada, Y. Sato, N. Takahashi, and Y. Kamio.** 1999. Functions of two types of NADH oxidases in energy metabolism and oxidative stress of *Streptococcus mutans*. J. Bacteriol. **181:**5940–5947.
20. **Hoefnagel, M. H., M. J. Starrenburg, D. E. Martens, J. Hugenholtz, M. Kleerebezem, S. Van II, R. Bongers, H. V. Westerhoff, and J. L. Snoep.** 2002. Metabolic engineering of lactic acid bacteria, the combined approach: kinetic modelling, metabolic control and experimental analysis. Microbiology **148:**1003–1013.
21. **Hols, P., A. Ramos, J. Hugenholtz, J. Delcour, W. M. de Vos, H. Santos, and M. Kleerebezem.** 1999. Acetate utilization in *Lactococcus lactis* deficient in lactate dehydrogenase: a rescue pathway for maintaining redox balance. J. Bacteriol. **181:**5521–5526.
22. **Hugenholtz, J., and M. Kleerebezem.** 1999. Metabolic engineering of lactic acid bacteria: overview of the approaches and results of pathway rerouting involved in food fermentations. Curr. Opin. Biotechnol. **10:**492–497.
23. **Hugenholtz, J., M. Kleerebezem, M. Starrenburg, J. Delcour, W. de Vos, and P. Hols.** 2000. *Lactococcus lactis* as a cell factory for high-level diacetyl production. Appl. Environ. Microbiol. **66:**4112–4114.
24. **Jensen, N. B., C. R. Melchiorsen, K. V. Jokumsen, and J. Villadsen.** 2001. Metabolic behavior of *Lactococcus lactis* MG1363 in microaerobic continuous cultivation at a low dilution rate. Appl. Environ. Microbiol. **67:**2677–2682.
25. **Jünemann, S., P. J. Butterworth, and J. M. Wrigglesworth.** 1995. A suggested mechanism for the catalytic cycle of cytochrome bd terminal oxidase based on kinetic analysis. Biochemistry **34:**14861–14867.
26. **Kandler, O.** 1983. Carbohydrate metabolism in lactic acid bacteria. Antonie Leeuwenhoek **49:**209–224.
27. **Lopez de Felipe, F., M. Kleerebezem, W. M. de Vos, and J. Hugenholtz.** 1998. Cofactor engineering: a novel approach to metabolic engineering in *Lactococcus lactis* by controlled expression of NADH oxidase. J. Bacteriol. **180:**3804–3808.
28. **Lopez de Felipe, F., M. J. C. Starrenburg, and J. Hugenholtz.** 1997. The role of NADH-oxidation in acetoin and diacetyl production from glucose in *Lactococcus lactis* subsp. *lactis* MG1363. FEMS Microbiol. Lett. **156:**15–19.
29. **Mason, P. W., D. P. Carbone, R. A. Cushman, and A. S. Waggoner.** 1981. The importance of inorganic phosphate in regulation of energy metabolism of *Streptococcus lactis*. J. Biol. Chem. **256:**1861–1866.
30. **Meiattini, F.** 1988. Inorganic peroxides, p. 566–571. *In* H. U. Bergmeyer, J. Bergmeyer, and M. Graßl (ed.), Methods of enzymatic analysis, 3rd ed., vol. 7. Verlag-Chemie, Weinheim, Germany.
31. **Neves, A. R., R. Ventura, N. Mansour, C. Shearman, M. J. Gasson, C. Maycock, A. Ramos, and H. Santos.** 2002. Is the glycolytic flux in *Lactococcus lactis* primarily controlled by the redox charge? Kinetics of NAD^+ and NADH pools determined *in vivo* by 13C-NMR. J. Biol. Chem. **277:**28088–28098.

32. **Neves, A. R., A. Ramos, M. C. Nunes, M. Kleerebezem, J. Hugenholtz, W. M. de Vos, J. Almeida, and H. Santos.** 1999. *In vivo* nuclear magnetic resonance studies of glycolytic kinetics in *Lactococcus lactis*. Biotechnol. Bioeng. **64:** 200–212.
33. **Neves, A. R., A. Ramos, C. Shearman, M. J. Gasson, J. S. Almeida, and H. Santos.** 2000. Metabolic characterization of *Lactococcus lactis* deficient in lactate dehydrogenase using in vivo ^{13}C-NMR. Eur. J. Biochem. **267:**3859–3868.
34. **Poolman, B., and W. N. Konings.** 1988. Relation of growth of *Streptococcus lactis* and *Streptococcus cremoris* to amino acid transport. J. Bacteriol. **170:** 700–707.
35. **Poolman, B., E. J. Smid, H. Veldkamp, and W. N. Konings.** 1987. Bioenergetic consequences of lactose starvation for continuously cultured *Streptococcus cremoris*. J. Bacteriol. **169:**1460–1468.
36. **Sanders, J. W., K. J. Leenhouts, A. J. Haandrikman, G. Venema, and J. Kok.** 1995. Stress response in *Lactococcus lactis*: cloning, expression analysis, and mutation of the lactococcal superoxide dismutase gene. J. Bacteriol. **177:** 5254–5260.
37. **Santos, H., and D. L. Turner.** 1986. Characterization of the improved sensitivity obtained using a flow method for oxygenating and mixing cell suspensions in NMR. J. Magnet. Reson. **68:**345–349.
38. **Schäfer, T., and P. Schönheit.** 1992. Maltose fermentation to acetate, CO_2 and H_2 in the anaerobic hyperthermophilic archaeon *Pyrococcus furiosus*: evidence for the operation of a novel sugar fermentation pathway. Arch. Microbiol. **158:**188–202.
39. **Schoberth, S. M., and A. A. de Graaf.** 1993. Use of *in vivo* ^{13}C nuclear magnetic resonance spectroscopy to follow sugar uptake in *Zymomonas mobilis*. Anal. Biochem. **210:**123–128.
40. **Smart, J., and T. D. Thomas.** 1987. Effect of oxygen on lactose metabolism in lactic streptococci. Appl. Environ. Microbiol. **53:**533–541.
41. **Snoep, J. L., M. J. Teixeira de Mattos, M. J. Starrenburg, and J. Hugenholtz.** 1992. Isolation, characterization, and physiological role of the pyruvate dehydrogenase complex and alpha-acetolactate synthase of *Lactococcus lactis* subsp. *lactis* bv. *diacetylactis*. J. Bacteriol. **174:**4838–4841.
42. **Thomas, T. D.** 1976. Activator specificity of pyruvate kinase from lactic streptococci. J. Bacteriol. **125:**1240–1242.
43. **van Kranenburg, R., J. D. Marugg, S. Van II, N. J. Willem, and W. M. de Vos.** 1997. Molecular characterization of the plasmid-encoded *eps* gene cluster essential for exopolysaccharide biosynthesis in *Lactococcus lactis*. Mol. Microbiol. **24:**387–397.
44. **Zitzelsberger, W., F. Götz, and K. H. Schleifer.** 1984. Distribution of superoxide dismutases, oxidases, and NADH peroxidase in various streptococci. FEMS Microbiol. Lett. **21:**243–246.